J Solid State Electrochem (2012) 16:75–82
DOI 10.1007/s10008-010-1280-9

ORIGINAL PAPER

Electrochemical oxidation behavior of 2,4-dinitrophenol at hydroxylapatite film-modified glassy carbon electrode and its determination in water samples

Huanshun Yin · Yunlei Zhou · Ruixia Han · Yanyan Qiu · Shiyun Ai · Lusheng Zhu

Received: 7 September 2010 / Revised: 5 December 2010 / Accepted: 12 December 2010 / Published online: 30 December 2010

Abstract Hydroxylapatite (HAP)-modified glassy carbon electrode (GCE) was fabricated and used to investigate the electrochemical oxidation behavior of 2,4-dinitrophenol (2,4-DNP) by cyclic voltammetry, differential pulse voltammetry, and chronocoulometry. The oxidation peak current of 2,4-DNP at the modified electrode was obviously increased compared with the bare GCE, indicating that HAP exhibits a remarkable enhancement effect on the electrochemical oxidation of 2,4-DNP. Based on this, a sensitive and simple electrochemical method was proposed for the determination of 2,4-DNP. The effects of HAP concentration, accumulation time, accumulation potential, pH, and scan rate were examined. Under optimal conditions, the oxidation peak current of 2,4-DNP was proportional to its concentration in the range from 2.0×10^{-6} to 6.0×10^{-4} M with a correlation coefficient of 0.9987. The detection limit was 7.5×10^{-7} M ($S/N = 3$). The proposed method was further applied to determine 2,4-DNP in water samples with recoveries from 96.75% to 106.50%.

Keywords 2,4-Dinitrophenol · Hydroxylapatite · Electrochemistry oxidation · Determination · Water sample

H. Yin · R. Han · Y. Qiu · S. Ai (✉)
College of Chemistry and Material Science,
Shandong Agricultural University,
Taian,
271018 Shandong, China
e-mail: ashy@sdau.edu.cn

L. Zhu
e-mail: lushzhu@sdau.edu.cn

H. Yin · L. Zhu (✉)
College of Resources and Environment,
Shandong Agricultural University,
Taian,
271018 Shandong, China

Y. Zhou
College of Life Science, Beijing Normal University,
100875 Beijing, China

Introduction

2,4-Dinitrophenol (2,4-DNP) is widely used in the production of dyes, pesticides developer, preservative, and indicator. Therefore, it is inevitable that 2,4-DNP will be released into the environment to cause pollution in the preparation and application process. Moreover, it has been proven that 2,4-DNP is highly toxic to humans, animals, and plants [1, 2]. The increasing use of 2,4-DNP requires a simple, sensitive, and selective detection technique to monitor its concentration due to its stability and persistence in the environment.

Up to now, many analytical methods, such as spectrophotometry [3], enzyme-linked immunosorbent assay (ELISA) [4], fluorescent detection [5], high-performance liquid chromatography (HPLC) [6], HPLC with electrochemical detection (HPLC-ED) [7], and capillary electrophoresis microchips with amperometric detection (CEMAD) [8], were investigated in terms of their suitability to determine trace amounts of 2,4-DNP. Although these techniques have the advantages of high sensitivity and selectivity, these techniques are time-consuming, expensive, and intricate. In addition, complicated instruments and skilled operators are also required. Therefore, they are unsuitable for on-line or field monitoring. Electrochemical methods should be a promising alternative for determining 2,4-DNP due to the advantages of simple operation, fast response, cheap instrument, low consumption, time-saving

feature, and in situ determination [9]. However, direct detection of 2,4-DNP using the bare electrode is rare because the response of 2,4-DNP at the bare electrode is poor. Based on this, chemically modified electrodes (CMEs) are widely studied for their high sensitivity. For the preparation of CMEs, one of the key aspects is to synthesize or find the modified material which can increase the current response. Hydroxylapatite (HAP) is a naturally occurring mineral mined for phosphoric acid production, which is mainly known for its special ability to contact bone tissue. In fact, HAP is an excellent sorbent for proteins, inorganic cations, and organic phenols [10, 11]. Recently, it has been proven that HAP is also a good electrode-modified material due to its excellent adsorption property. For instance, Hanane et al. used the HAP-modified platinum electrode to determine lead (II) in water. The detection limit was achieved at 0.5 μM [12]. El Mhammedi et al. prepared HAP-modified carbon paste electrode to determine 4-nitrophenol. It was demonstrated that 4-nitrophenol can be adsorbed onto the HAP surface to increase the current response. The detection limit was estimated to be 8 nM [13]. In addition, the HAP-modified carbon paste electrode also showed an excellent electrochemical response for cadmium [14] and Paraquat [15].

In this work, hydroxylapatite-modified glassy carbon electrode was fabricated and the electrochemical oxidation behavior of 2,4-DNP was investigated using this modified electrode. The effect factors, such as HAP concentration, pH, scan rate, accumulation time, and accumulation potential, were optimized. The proposed method was further applied to determine the trace amounts of 2,4-DNP in water samples.

Experimental

Reagents and apparatus

HAP and 2,4-DNP were purchased from Aladdin Reagent Co., Ltd. (China) and used as received. A 0.1-M 2,4-DNP stock solution was prepared with anhydrous ethanol and kept in darkness at 4 °C in a refrigerator. Working solutions were freshly prepared before use by diluting the stock solution. Phosphate buffer solution (PBS) was prepared by mixing the stock solution of 0.1 M NaH_2PO_4 and 0.1 M Na_2HPO_4 and adjusting the pH with HCl or NaOH. Other chemicals were of analytical reagent grade and all solutions were prepared with double-distilled deionized water from quartz.

Electrochemical experiments were performed with CHI660C electrochemical workstation (Shanghai Chenhua Co., China) with a conventional three-electrode cell. A bare or HAP-modified GCE (CHI104, d = 3 mm) was used as working electrode. A saturated calomel electrode and a platinum wire were used as reference electrode and auxiliary electrode, respectively. The pH measurements were carried out on PHS-3 C exact digital pH meter (Shanghai KangYi Co. Ltd., China), which was calibrated with standard pH buffer solutions. The transmission electron microscope (TEM) image was obtained at JEOL-1200EX TEM (Japan). The image of scanning electron microscope (SEM) was obtained at JSM-6610LV (Japan). All the measurements were carried out at room temperature.

Preparation of HAP film electrode

A glassy carbon electrode was polished to a mirror-like finish with 0.3- and 0.05-μm alumina slurry on a micro-cloth pad and cleaned thoroughly in an ultrasonic cleaner with double-distilled deionized water, anhydrous ethanol, and double-distilled deionized water, sequentially. Then, the electrode was dried under nitrogen blowing before use.

For the preparation of HAP film-modified GCE, 6 mg HAP was first added into 1 mL double-distilled deionized water, followed by ultrasonication for 1 h to obtain a homogeneously dispersed solution. Then, 5 μL of HAP suspension was deposited on the freshly prepared GCE surface. After the solvent was evaporated, the electrode surface was thoroughly rinsed with double-distilled deionized water to wash away the unimmobilized modifier. The obtained electrode was noted as HAP/GCE. The modified electrodes were stored at 4 °C in a refrigerator when not in use.

Electrochemical measurements

Unless otherwise stated, 0.1 M pH 7.0 PBS was used as the supporting electrolyte for 2,4-DNP analysis. The voltammetric determination of 2,4-DNP was performed in an electrochemical cell with 10 mL of 0.1 M pH 7.0 PBS. The accumulation step was carried out at −0.10 V for 330 s with stirring, and then the cyclic voltammograms and differential pulse voltammograms were recorded from 0.40 to 1.40 V. The oxidation peak current measured at 1.184 V in differential pulse voltammograms was applied for the quantification of 2,4-DNP.

Results and discussion

Characterization of HAP/GCE

Figure 1a was the TEM image of HAP, which showed that most of the particles are quite uniform, spindle-like structures which are 100–200 nm in length and 20–40 nm in width. The typical morphologies of GCE (b) and HAP/

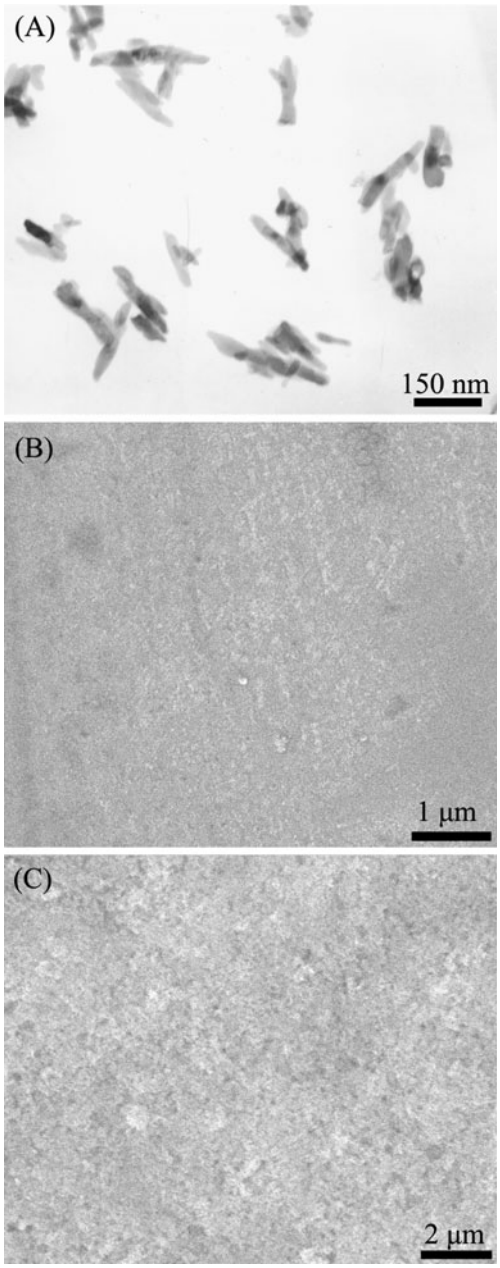

Fig. 1 **a** TEM image of HAP. SEM images of GCE (**b**) and HAP/GCE (**c**)

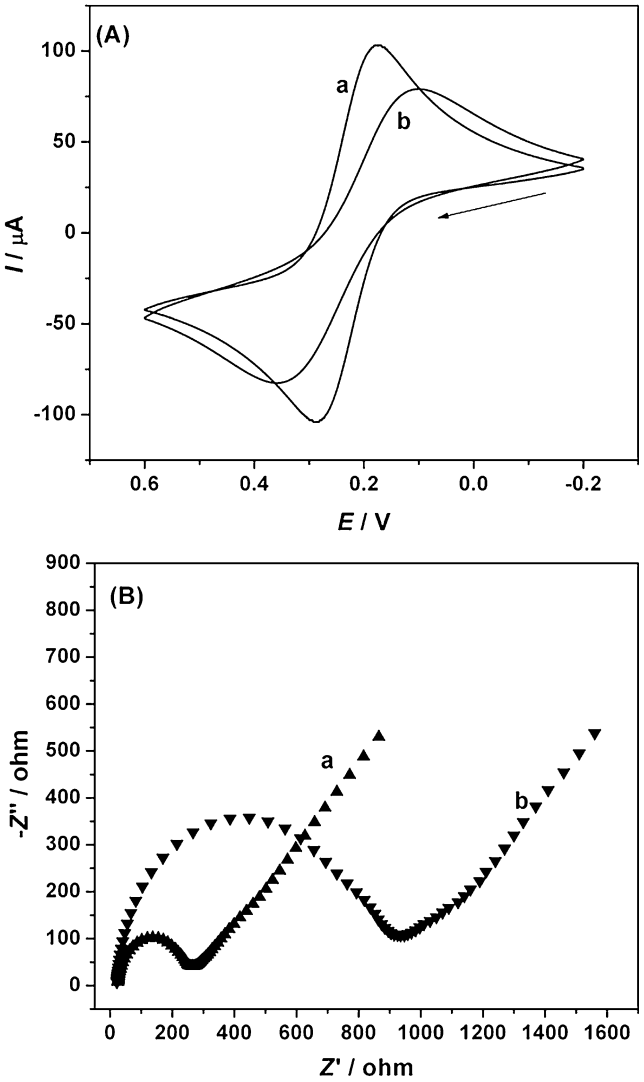

Fig. 2 **a** Cyclic voltammograms at GCE (*a*) and HAP/GCE (*b*) in 5 mM $Fe(CN)_6^{3-/4-}$ (1:1) solution containing 1 M KCl. Scan rate, 100 mV s^{-1}. **b** Nyquist plots of GCE (*a*) and HAP/GCE (*b*) in 5 mM $Fe(CN)_6^{3-/4-}$ (1:1) solution containing 1 M KCl. The frequency range was from 10^{-1} to 10^5 Hz at the formal potential of 0.237 V

GCE (c) were also shown in Fig. 1. It can be seen that the GCE surface appeared as a flat surface with small holes. When HAP was immobilized on the GCE surface, an irregular and porous surface was observed. This porous film could extremely enhance the active surface area of GCE.

The electrochemical properties of HAP/GCE were investigated using $[Fe(CN)_6]^{3-/4-}$ as electrochemical probes. Figure 2a showed the cyclic voltammograms of 5 mM $[Fe(CN)_6]^{3-/4-}$ in 1.0 M KCl solution at the bare GCE and HAP/GCE. At the bare GCE (curve a), a pair of well-defined redox peak was observed. However, the redox peak current obviously decreased and the peak-to-peak separation shifted positively at HAP/GCE, which can be attributed to the HAP film deposited onto the surface of GCE. The electronegative hydroxyl and phosphate ion may act as the blocking layer for the diffusion of $[Fe(CN)_6]^{3-/4-}$ into the film and hindered the electron and mass transfer. To further investigate the electrochemical behavior of HAP/GCE, the electrochemical impedance spectra were used. Figure 2b presented the Nyquist diagrams of bare GCE (a) and HAP/GCE (b) in 5 mM $[Fe(CN)_6]^{3-/4-}$ containing 1 M KCl. The bare GCE (curve a) showed a small, well-defined semi-circle at higher frequencies, indicating small electron transfer impedance. Nevertheless, a big semi-circle was observed at HAP/GCE, indicating that the impedance value

increased significantly, which can be attributed to the immobilized HAP film, increasing the interface resistance of the electrode/solution system, leading to a lower rate of the electron transfer of $Fe(CN)_6^{3-/4-}$. This phenomenon also demonstrates that HAP was successfully immobilized on the GCE surface.

Electrochemical oxidation behaviors of 2,4-DNP

The electrochemical oxidation behavior of 2,4-DNP was studied using cyclic voltammetry in 0.1 M, pH 7.0, PBS. Figure 3 illustrated the cyclic voltammograms of GCE (a, c) and HAP/GCE (b, d) in the absence (a, b) and presence (c, d) of 0.2 mM 2,4-DNP containing 0.1 M, pH 7.0, PBS. It can be seen that no redox peak was observed in the absence of 2,4-DNP on HAP/GCE, indicating that HAP is an electrochemically inactive compound in the selected potential region. When 2,4-DNP was added into PBS, a well-defined oxidation peak was observed at HAP/GCE with the oxidation potential of 1.255 V after 330 s of accumulation at −0.1 V. It is not difficult to believe that this phenomenon should be attributed to the oxidation of 2,4-DNP. However, no corresponding reduction peak was observed in the following reverse scan from 1.4 to 0.4 V, indicating that the oxidation of 2,4-DNP is a totally irreversible electrode process under the above experimental conditions. Compared with bare GCE, the oxidation peak current of 2,4-DNP obtained at HAP/GCE obviously increased and the corresponding oxidation peak potential decreased (1.255 V at HAP/GCE and 1.271 V at GCE), which could be attributed to the immobilized HAP on the electrode surface, increasing the adsorption of 2,4-DNP onto the electrode surface, improving the electron transfer rate, and enhancing the electrochemical oxidation response. However, during the following successive cyclic sweeps, the oxidation peak current decreased greatly and the oxidation peak potential shifted positively (data not shown). It resulted from the fact that the electrode surface is blocked by the adsorption of the oxidation products of 2,4-DNP which reduce the effective reaction sites at the modified electrode surface. Therefore, the oxidation peak current in the first cyclic sweep was recorded for 2,4-DNP analysis in the following studies. In addition, because the preparation of the modified electrode is very simple and the preparation reproducibility was satisfactory under the same experiment conditions (see "Calibration curve"), the fabricated electrode was only used to scan for one time. It has also been reported that 2,4-DNP can be determined using the reduction signal because the two nitryls ($–NO_2$) in the benzene ring of the 2,4-DNP molecule can be electrochemically reduced to from two hydroxylamino groups (–NHOH) [16–18]. Therefore, the electrochemical reduction behavior of 2,4-DNP was investigated at HAP/GCE by differential pulse voltammetry in 0.1 M, pH 7.0, PBS. The result indicated that 2,4-DNP showed two sensitive reduction peaks at −0.648 and −0.796 V. However, the two peaks can be easily interfered by some common metal ions, such as Pb^{2+} and Cd^{2+}, because their reduction peak potentials (Pb^{2+}, −0.664 V; Cd^{2+}, −0.854 V) are close to the reduction peaks of 2,4-DNP. However, the oxidation signal of 2,4-DNP will not be interfered by the above two metal ions. Considering the determination selectivity, the oxidation signal of 2,4-DNP was used in this work.

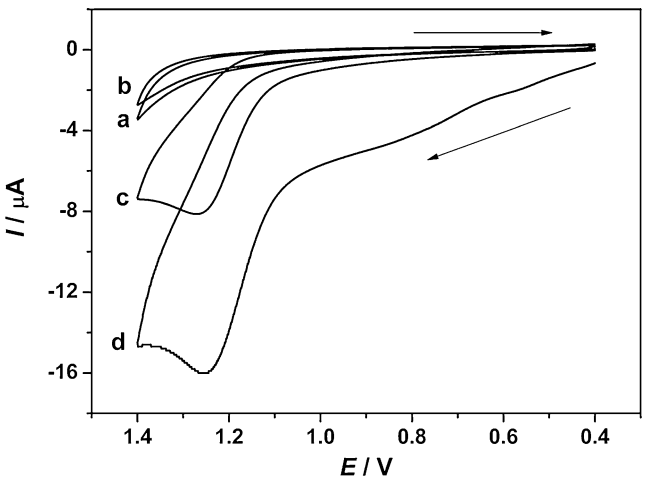

Fig. 3 Cyclic voltammograms at GCE (*a*, *c*) and HAP/GCE (*b*, *d*) in the absence (*a*, *b*) and presence (*c*, *d*) of 0.2 mM 2,4-DNP in 0.1 M PBS (pH 7.0). Scan rate, 100 mV/s. Accumulation time, 330 s. Accumulation potential, −0.1 V

In order to calculate the electron number (n) involved in the 2,4-DNP oxidation process at HAP/GCE, the n value was determined by cyclic voltammogram using the following equation [19]:

$$\alpha n = \frac{47.7}{E_p - E_{p/2}} \quad (1)$$

where E_p and $E_{p/2}$ represent the peak potential and the potential at which $I = I_p/2$ in cyclic voltammogram, respectively. In this work, E_p = 1.238 mV and $E_{p/2}$ = 1.161 mV. Therefore, αn was calculated to be 0.62. Generally, α (charge transfer coefficient) is assumed to be 0.5 in totally irreversible electrode process. So, n was calculated to be 1.24 ≈ 1. That is to say, one electron takes part in the electrochemical oxidation process.

Optimization of experimental conditions

The effect of the amount of HAP on the oxidation peak current of 0.1 mM 2,4-DNP was investigated. The 5-μL HAP suspensions with different concentrations were deposited onto the GCE surface, and then the cyclic voltammograms were recorded. As can be seen in Fig. 4a, the maximum current

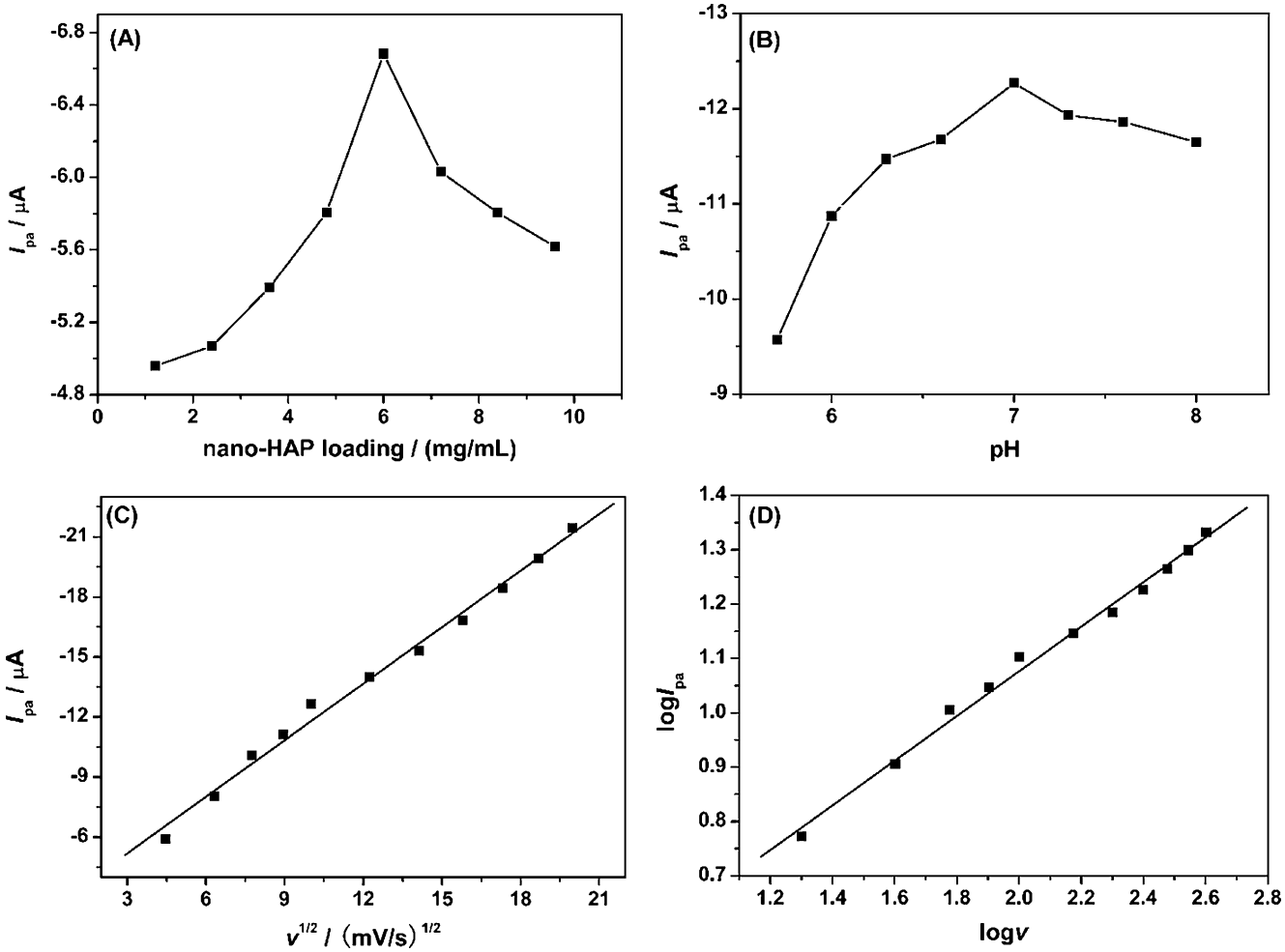

Fig. 4 **a** Effects of HAP loading on the oxidation peak current of 0.1 mM 2,4-DNP in 0.1 M PBS. **b** Effects of pH on the oxidation peak current of 2,4-DNP. **c** Dependence of the oxidation peak current on the square root of scan rate. **d** Relationship between the logarithm of peak potential and logarithm of scan rate

response was obtained at the concentration of 6 mg mL^{-1}. After that concentration, it decreased. This is related to the thickness of the HAP film. If the film was too thin, the adsorption sites were insufficient, leading to a weak adsorption for 2,4-DNP, resulting in the small oxidation peak current. If it was too thick, the film conductivity was reduced to block the electron transfer and decrease the oxidation peak current. Therefore, 6 mg mL^{-1} HAP suspension was used in the following investigations.

The effect of accumulation time on the oxidation peak current of 0.1 mM 2,4-DNP was studied with the accumulation potential of −0.10 V. When the accumulation time improves from 0 to 330 s, the oxidation peak current linearly increased. Then, the oxidation peak current increased slightly with an extension in the accumulation time, suggesting that the amount of 2,4-DNP adsorbed at the HAP film tends to be a saturated value. Therefore, 330 s was chosen as the optimal accumulation time. On the other

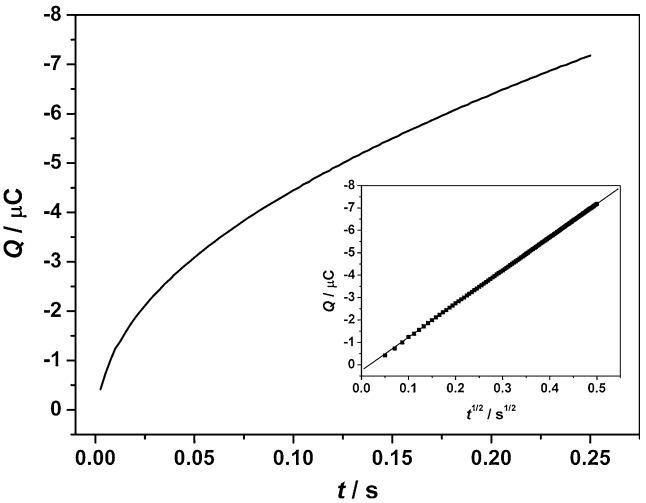

Fig. 5 Plot of Q–t curves of HAP/GCE after point-by-point background subtraction in 0.1 M PBS containing 0.1 mM 2,4-DNP. *Insert*, plot of Q–$t^{1/2}$ curves on HAP/GCE

Scheme 1 The possible mechanism of 2,4-DNP oxidation at HAP/GCE

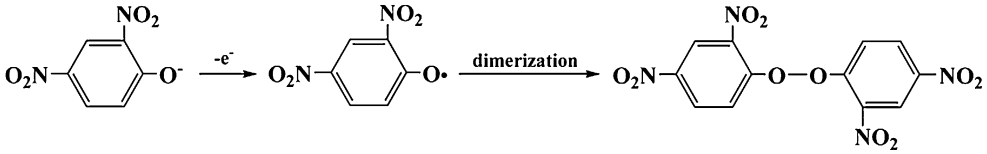

hand, the influence of accumulation potential on the oxidation of 2,4-DNP was also investigated in 0.1 mM 2,4-DNP with a fixed accumulation time of 330 s. The oxidation peak current increased when accumulation potential shifted from 0.90 to −0.10 V and then decreased when the accumulation potential became more negative. Thus, −0.10 V was used for subsequent determination.

The effect of pH on the electrochemical oxidation response of 0.4 mM 2,4-DNP was investigated by cyclic voltammetry. The relationship between peak current and peak potential against pH over the range of 5.7 to 8.0 was shown in Fig. 4b. With increasing pH from pH 5.7 to 7.0, the oxidation peak current also increased because HAP can slowly dissolve in an acidic solution and lose its ability for adsorbing 2,4-DNP [13]. However, the oxidation peak current decreased when the solution pH was higher than 7.0. It has been reported that the pK_a of 2,4-DNP is 4.097 [9]. 2,4-DNP can completely ionize to form 2,4-dinitrophenoxy anion when the solution pH is higher than its pK_a. By means of accumulation, 2,4-dinitrophenoxy anion was adsorbed on the electrode surface to generate a electrochemical signal. However, the concentration of hydroxyl anion increases rapidly when pH > 7, which might result in a lower affinity of 2,4-DNP toward HAP and decrease the adsorption amount of 2,4-DNP. Considering the determination sensitivity, pH 7.0 was chosen for the subsequent analytical experiments. Moreover, the oxidation potential was almost unchanged when the pH changed from 5.7 to 8.0, indicating that no proton was involved in the oxidation process.

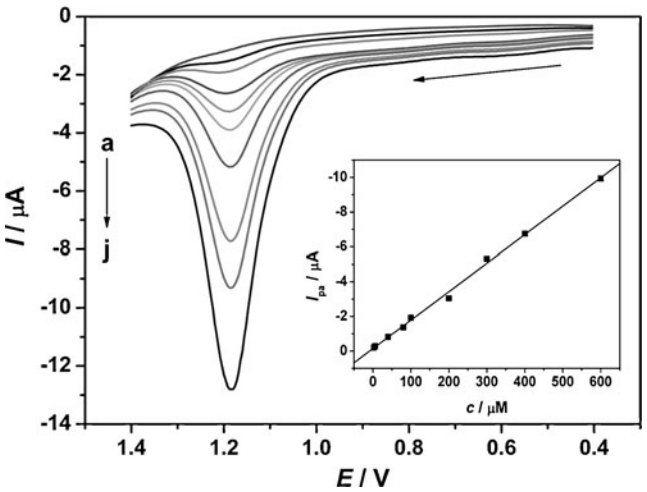

Fig. 6 Differential pulse voltammograms at HAP/GCE in 2,4-DNP solution at different concentrations. *a–j*, 0, 2, 6, 40, 80, 100, 200, 300, 400, and 600 μM. *Insert*, calibration curve for 2,4-DNP

Figure 4c illustrated the effect of scan rate on the electrochemical oxidation peak current of 0.4 mM 2,4-DNP at HAP/GCE. It is clear that there is a good linear relationship between the oxidation peak current and the square root of scan rate. The regression equation can be expressed as $I_{pa} = -0.94v^{1/2} - 2.37$ (μA, mV/s, $R = 0.9959$), indicating that the electrode oxidation process is controlled by diffusion rather than adsorption. In addition, there was a linear relation between log I_{pa} and log v, corresponding to the following equation: log I_{pa} = 0.41 log v + 0.25 (μA, mV/s, $R = 0.9967$) (shown in Fig. 4d). The slope of 0.41 is close to the theoretically expected value of 0.5 for a diffusion-controlled process [20]. It seemed to be inconsistent with the accumulation characteristics of 2,4-DNP mentioned above. This may relate to the diffusion of 2,4-DNP accumulated in the HAP film to the electrode surface to undergo electrochemical reaction. A similar phenomenon was also observed in the previous report for the cathodic reduction of methylparathion [21].

Chronocoulometry

Chronocoulometry was used to investigate the diffusion coefficient (D) of 2,4-DNP at nano-HAP/GCE. The D can be calculated using the equation given by Anson as follows [22]:

$$Q(t) = \frac{2nFAcD^{1/2}t^{1/2}}{\pi^{1/2}} + Q_{dl} + Q_{ads} \quad (2)$$

where A is the surface area of the working electrode, c is the concentration of substrate, D is the diffusion coefficient, Q_{dl} is the double layer charge which could be eliminated by background subtraction, and Q_{ads} is the Faradaic charge. Other symbols have their usual meaning. As shown in the inset of Fig. 5, the plot of charge (Q) against the square root of time ($t^{1/2}$) showed a linear relationship with the slope of 1.49×10^{-5} C/s$^{1/2}$ and Q_{ads} of 2.53×10^{-7} C after background subtraction. As $n = 1$, $A = 0.07$ cm^2 (geometric area) and $c = 0.1$ mM, it was calculated that $D = 3.81 \times 10^{-4}$ cm^2/s. In addition, according to the equation of $Q_{ads} = nFA\Gamma_s$, the adsorption capacity, Γ_s, can be obtained as $3.75 \times$

Table 1 Performance comparison of HAP/GCE for 2,4-DNP detection with other methods

Method	Linear range (μM)	LOD (μM)	References
ELISA[a]	0.00395–0.0526	0.00187	[4]
Hanging mercury drop electrode	0.36–5.75	0.00935	[25]
Fluorescent detection	–	0.036	[5]
HPLC[b]	5–250	1	[26]
m-AgSAE[c]	2–10	1.8	[17]
p-AgSAE[d]	2–10	5.8	[17]
HPLC-ED[e]	5–2,500	5	[7]
HPLC-ED[f]	10–2,500	10	[7]
CEM-AD[g]	–	10	[8]
Pt–Ag/AgCl electrode	100–3,000	85	[27]
HAP/GCE	2–600	0.75	This work

[a] Enzyme-linked immunosorbent assay

[b] High-performance liquid chromatography

[c] Mercury meniscus-modified silver solid amalgam electrode

[d] Liquid mercury-free polished silver solid amalgam electrode

[e] High-performance liquid chromatography with electrochemical detection (thin-layer detector)

[f] High-performance liquid chromatography with electrochemical detection (wall-jet detector)

[g] Capillary electrophoresis microchips with amperometric detection

10^{-11} mol/cm^2, indicating that nano-HAP has an excellent adsorption property towards 2,4-DNP.

Mechanism studies

From the research results obtained in cyclic voltammetry and pH effect, one can conclude that the electrochemical oxidation process of 2,4-DNP is a one-electron process. No proton was involved in this process. Therefore, in the light of the results obtained in this work and in voltammetry studies undertaken by other researchers [23, 24], the possible oxidation mechanism was expressed as shown in Scheme 1. It is well known that the pK_a of 2,4-DNP is 4.097. The optimal pH in this work is 7.0; thus, the absorbed 2,4-DNP should be anion. The 2,4-dinitrophenoxy nion was oxidized to form a 2,4-dinitrophenoxy radical, which can undergo dimerization. The formation of a dimer is nonconducting and it can block the further oxidation of 2,4-DNP at the electrode surface, which was testified by the successive cyclic sweeps, resulting in the decrease of oxidation peak current and increase of oxidation peak potential.

Calibration curve

For the purpose of developing a sensitive and reliable voltammetric method for determining 2,4-DNP, differential pulse voltammetry was selected due to the low background current and high sensitivity. As can be seen in the insert of Fig. 6, under the optimum conditions, a linear relationship between the oxidation peak current and 2,4-DNP concentration was obtained in the range from 2 to 600 μM. The regression equation can be expressed as $I_{pa} = -0.016c - 0.14$ (μA, μM, $R = 0.9987$). The detection limit was evaluated to be 0.75 μM ($S/N = 3$). The determination performance of HAP/GCE was compared with that of other methods and the results were listed in Table 1. It is clear that the linear range of HAP/GCE is wider and the detection limit is lower than that of some methods. Though the detection limit of HAP/GCE is higher than ELISA [4], hanging mercury drop electrode [25], and fluorescent detection [5], ELISA requires an expensive biological reagent (goat anti-rabbit IgG coupled to horseradish peroxidase) and a dangerous chemical reagent (NaN_3), hanging mercury drop electrode would need poisonous mercury, and fluorescent detection would need a costly reagent and instrument. Therefore, the fabricated electrode is suitable for the determination of 2,4-DNP with the advantages of easy fabrication, simple operation, cheap and small-sized instrument, and real-time determination.

From the calibration curve studies, another kinetic parameter, reaction order, can also be obtained based on the slope of the plot of the logarithm of 2,4-DNP concentration (log c) versus the logarithm of the corresponding oxidation peak current (log I_{pa}). There was a linear relationship between log c and log I_{pa} with the regression equation of $\log I_{pa} = 0.94 \log c - 1.61$ (μA, μM, $R = 0.9968$). The slope is 0.94, indicating that the

Table 2 Determination of 2,4-DNP in water samples

Samples	Added (μM)	Found (μM)	RSD (%)	Recovery (%)
Tap water	6.0	5.87	4.52	97.83
Lake water	6.0	6.29	3.84	104.83
River water	6.0	6.21	3.15	103.5
Waste water	6.0	6.33	4.37	105.5

electrochemical oxidation of 2,4-DNP at HAP/GCE follows the first-order kinetics with respect to 2,4-DNP [28].

The possible interferences of other species on the determination of 2,4-DNP were examined. It was found that 1,000-fold concentrations of Na^+, Ca^{2+}, Mg^{2+}, Fe^{3+}, ,Al^{3+}, Zn^{2+}, Ni^{2+}, Cu^{2+}, F^-, Cl^-, SO_4^{2-}, SO_3^{2-}, CO_3^{2-}, PO_4^{3-}, and NO_3^- and 200-fold concentrations of phenol, pyrocatechol, hydroquinone, resorcinol, *p*-aminophenol, *o*-aminophenol, *p*-chlorophenol, *o*-chlorophenol, *o*-nitrobenzoic acid, *m*-nitrobenzoic acid, and *p*-nitrobenzoic acid do not interfere with the oxidation signal of 10 μM 2,4-DNP (peak current change <8%). However, it was also found that 100 μM of 2-nitrophenol (peak current change, 23.24%) and 4-nitrophenol (peak current change, 24.01%) interfere with the determination.

The stability of the HAP/GCE was evaluated by measuring the oxidation peak current of 10 μM 2,4-DNP every 5 days. In the determination interval, the electrodes were stored at 4 °C in a refrigerator. The results showed that the electrode could retain 91.48% of its original response after 10 days, suggesting acceptable storage stability. The fabricated reproducibility was also investigated by determining the oxidation peak current of 10 μM 2,4-DNP. The RSD for the six modified electrodes prepared independently was 4.87%, implying that this method has good reproducibility.

Analytical application

The proposed method was used to determine 2,4-DNP in water samples, which were collected from Taian of Shandong Province, China. The samples were first filtered, and then the content of 2,4-DNP was determined by the standard addition method. Each sample was determined for three times. The results were listed in Table 2. The RSD was below 5.0% and the recoveries were in the range from 96.75% to 106.50%, indicating that the proposed method should be reliable, effective, and sufficient for 2,4-DNP determination.

Conclusion

In this work, a hydroxylapatite-modified glassy carbon electrode has been successfully developed for the electrochemical oxidation determination of 2,4-DNP in PBS. Hydroxylapatite showed the obvious adsorption capacity towards 2,4-DNP, characterized by the enhancement of the oxidation peak current. Under optimum conditions, the modified electrode was successfully used to determine 2,4-DNP in water samples with satisfactory results. Moreover, the electrode fabrication is very simple, and the modified material was very cheap and easily obtained. Based on these, a promising electrochemical method was developed for 2,4-DNP determination in water samples.

Acknowledgements This work was supported by the National Natural Science Foundation of China (No. 20775044) and the Natural Science Foundation of Shandong Province, China (Y2006B20).

Reference

1. Knox RC, Canter LW (1996) Water Air Soil Pollut 88:205–226
2. Harrison MAJ, Barra S, Borghesi D, Vione D, Arsene C, Iulian Olariu R (2005) Atmos Environ 39:231–248
3. Űzer A, Erçağ E, Apak R (2004) Anal Chim Acta 505:83–93
4. Oubiña A, Barceló D, Marco MP (1999) Anal Chim Acta 387:267–279
5. Carter RM, Blake RC, Nguyen TD, Bostanian LA (2003) Biosens Bioelectron 18:69–72
6. Berhanu T, Liu J, Romero R, Megersa N, Jnsson J (2006) J Chromatogr A 1103:1–8
7. Danhel A, Shiu K, Yosypchuk B, Barek J, Peckova K, Vyskocil V (2009) Electroanalysis 21:303–308
8. Fischer J, Barek J, Wang J (2006) Electroanalysis 18:195–199
9. Wang XG, Wu QS, Liu WZ, Ding YP (2006) Electrochim Acta 52:589–594
10. Dove GB, Mitra G, Roldan G, Shearer MA, Cho MS (2009) Protein Purification. American Chemical Society, Washington, DC, pp 194–209
11. Sheha RR (2007) J Colloid Interface Sci 310:18–26
12. Zejli H, Temsamani KR, Hidalgo-Hidalgo de Cisneros JL, Naranjo-Rodriguez I, Sharrock P (2006) Electrochem Commun 8:1544–1548
13. El Mhammedi MA, Achak M, Bakasse M, Chtaini A (2009) J Hazard Mater 163:323–328
14. El Mhammedi MA, Achak M, Najih R, Bakasse M, Chtaini A (2009) Mater Chem Phys 115:567–571
15. El Mhammedi MA, Bakasse M, Chtaini A (2007) Electroanalysis 19:1727–1733
16. Fischer J, Barek J, Yosypchuk B, Navrátil T (2006) Electroanalysis 18:127–130
17. Fischer J, Vanourkova L, Danhel A, Vyskocil V, Cizek K, Barek J, Peckova K, Yosypchuk B, Navratil T (2007) Int J Electrochem Sci 2:226–234
18. Niaz A, Fischer J, Barek J, Yosypchuk B (2009) Electroanalysis 21:1786–1791
19. Bard AJ, Faulkner LR (2001) Electrochemical methods: fundamentals and applications, 2nd edn. Wiley, New York
20. Gosser DK (1993) Cyclic voltammetry: simulation and analysis of reaction mechanisms. VCH, New York
21. Fan S, Xiao F, Liu L, Zhao F, Zeng B (2008) Sensor Actuat B 132:34–39
22. Anson F (1964) Anal Chem 36:932–934
23. Alizadeh T, Ganjali MR, Norouzi P, Zare M, Zeraatkar A (2009) Talanta 79:1197–1203
24. Honeychurch KC, Hart JP (2007) Electroanalysis 19:2176–2184
25. Ni Y, Wang L, Kokot S (2001) Anal Chim Acta 431:101–113
26. Zhang W, Danielson N (2003) Anal Chim Acta 493:167–177
27. Khachatryan K, Smirnova S, Torocheshnikova I, Shvedene N, Formanovsky A, Pletnev I (2005) Anal Bioanal Chem 381:464–470
28. Cheng H, Scott K (2006) Electrochim Acta 51:3429–3433